Meridianiite detected in ice

F. Elif GENCELI,[1] Shinichirou HORIKAWA,[2] Yoshinori IIZUKA,[2] Toshimitsu SAKURAI,[2] Takeo HONDOH,[2] Toshiyuki KAWAMURA,[2] Geert-Jan WITKAMP[1]

[1]*Process Equipment Section, Delft University of Technology, Leeghwaterstraat 44, 2628 CA Delft, The Netherlands*
E-mail: e.genceli@hotmail.com
[2]*Institute of Low Temperature Science, Hokkaido University, Sapporo 060-0819, Japan*

ABSTRACT. Inclusions affect the behavior of ice, and their characteristics help us understand the formation history of the ice. Recently, a low-temperature magnesium sulfate salt was discovered. This paper describes this naturally occurring $MgSO_4 \cdot 11H_2O$ mineral, meridianiite, derived from salt inclusions in sea ice of Lake Saroma, Japan and in Antarctic continental core ice. Its occurrence is confirmed by using micro-Raman spectroscopy to compare Raman spectra of synthetic $MgSO_4 \cdot 11H_2O$ with those of the inclusions.

INTRODUCTION

Seasonal sea ice strongly modulates global climate and ecology through its effect on ocean albedo, ocean–atmosphere heat transfer and transfer of gases and particles (including nutrients) between the atmosphere and ocean. Small changes in the atmosphere/ocean/ice composition ratio may lead to significant changes in the nature of the sea-ice cover and its ecology. Investigations of mineral inclusions in sea ice are expected to provide insights which may help in climate studies. The presence of minerals in Antarctic ice will also provide significant information on past atmospheric compositions. The snowfall composition, buried over time, contains records of the climatic history in the ice, which might successfully be used in climate and environmental studies (Jouzel and others, 1989, 2006; Legrand and Mayewski, 1997; Petit and others, 1999; Jouzel, 2003; EPICA Communiy Members, 2004)

The aim of this work is to report the occurrence of inclusions of the recently discovered mineral meridianiite in sea ice and Antarctic continental ice.

The $MgSO_4 \cdot 11H_2O$ crystal structure is triclinic with space group P-1 (no. 2). $MgSO_4 \cdot 11H_2O$ had previously been described as $MgSO_4 \cdot 12H_2O$ by Fritzsche (1837). Through weight loss via dehydration, Fritzsche attempted to estimate the water content of salt, which led to an error by one water molecule. The $MgSO_4 \cdot 11H_2O$ crystal is colorless and needle-shaped with the parameters:

formula weight, FW = 318.55;

crystal size = $0.54 \times 0.24 \times 0.18\,mm^3$;

length of the unit cell dimension along the crystallographic *x* axis, a = 6.725 48(7) Å;

length of the unit cell dimension along the crystallographic *y* axis, b = 6.779(14) Å;

length of the unit cell dimension along the crystallographic *z* axis, c = 17.290(5) Å;

angle between the *y* and *z* crystallographic axes, $\alpha = 88.255(1)^\circ$;

angle between the *x* and *z* crystallographic axes, $\beta = 89.478(2)^\circ$;

angle between the *x* and *y* crystallographic axes, $\gamma = 62.598(1)^\circ$;

unit cell volume, $V = 699.54(3)\,Å^3$;

number of formula units in the crystallographic unit cell, $Z = 2$;

calculated density, $D_{calc} = 1.512\,g\,cm^{-3}$; and

absorption coefficient, $\mu = 0.343\,mm^{-1}$ (Genceli and others, 2007).

On Earth, epsomite ($MgSO_4 \cdot 7H_2O$) is present in, for example, crusts and efflorescences in coal or metal mines, limestone caves, oxidized zones of sulfide ore deposits, salt lakes and playas. In the laboratory, as well as in nature, $MgSO_4 \cdot 11H_2O$ crystallizes from a suspension around its eutectic point, i.e. concentrations between 17.3 and 21.4 wt% $MgSO_4$ and temperatures between –3.9 and 1.8°C (Genceli and others, 2007). If the temperature of the magnesium sulfate reservoir lies above 1.8°C, epsomite formation occurs instead of meridianiite.

Previously, Antarctic ice impurities were analysed using scanning electron microscopy and energy dispersive spectrometry (SEM/EDS) (Baker and Cullen, 2003; Barnes and Wolff, 2004). Later, Ohno and other (2006) used micro-Raman spectroscopy to examine micro-inclusions in polar ice from Dome Fuji in order to determine the salt composition. It was found that the inclusions mainly consisted of sulfate salts with small amounts of other soluble salts and insoluble dust (Ohno and others, 2005, 2006).

We have now made detailed studies of inclusions in sea ice and in Antarctic core ice by micro-Raman spectroscopy.

SAMPLING METHODS

Sea ice

Sea-ice samples were collected from Lake Saroma (Saroma-ko), the third largest lake in Japan, located on the north-eastern shore of Hokkaido island. The lake is a semi-enclosed embayment connected with two openings to the Sea of Okhotsk. Most of the lake surface is covered with sea ice during winter (Kawamura and others, 2004).

The sea-ice samples were selected from a core sampled at 44°07′ N, 143°57′ E in March 2006: core No. 06.03.07-St.4. The average sampling-day temperatures at the surface and at

sea level were –4.8 and –0.7°C, respectively. In this study, only the surface (top 1 cm) of the sea-ice core was analysed, as this layer was in direct contact with the air and was the coldest section. The lowest air and ice surface temperatures during March 2006 were –16.4 and –20.6°C, respectively, the average day temperature recorded was –3.9°C and the average ice surface temperature was –2.8°C (personal communication from T. Kawamura, 2007). The ice temperature was measured in situ immediately after extraction of the core, using calibrated Technol Seven, D617 thermistor probes (precision ±0.1°C) inserted into small, drilled holes with the exact diameter of the probe. After collection, the samples were stored at –15°C, at the Institute of Low Temperature Science, Hokkaido University.

During ice formation, the sea-water temperature near the ice decreases gradually while the remaining brine becomes increasingly saline. Since ice generally contains no salt in the ice body, the dissolved salts are rejected and remain in the adjacent sea water. However, a portion of the brine can become mechanically trapped in the ice matrix (Wakatsuchi and Kawamura, 1987). As cooling continues, different solid salts will crystallize from the entrapped brine at different temperatures (Weeks and Ackley, 1982). Crystallization of the salts from sea-ice brine at various temperatures was deduced from changes in brine composition and stability ranges of individual salts in the corresponding pure salt-water systems (Sinha, 1977). The solubility of one salt affects the solubility of the other.

As mentioned, the pure $MgSO_4$-H_2O aqueous system crystallizes in the $MgSO_4 \cdot 11H_2O$ form below +1.8°C and has a eutectic point at –3.9°C and 17.3 wt% $MgSO_4$ concentration (Genceli and others, 2007). Presence of impurities shifts the eutectic point to lower temperatures. Therefore, the formation path of $MgSO_4 \cdot 11H_2O$ from sea brine composition is not completely known, but it has been established here that inclusions of this salt were indeed present in the samples which were stored and measured at –15°C. Given that the lowest ice exposure air temperature during March 2006 was –16.4°C and the highest ice temperature was 0.2°C, it is reasonable to assume that the samples from the surface sea ice were kept intact during sampling and analysis.

Antarctic core ice

The ice core used in this study was collected from Dome Fuji station, East Antarctica (77°19′ S, 39°42′ E; 3810 m a.s.l.), near the summit of the east Dronning Maud Land plateau. The average snow temperature at 10 m depth is –58°C. For further information about the sampling, see Dome-F Deep Coring Group (1998). After collection, the samples were stored at –50°C, at the Institute of Low Temperature Science, Hokkaido University. In this work, samples from 362 m depth were analysed: core No. 03-124.

EXPERIMENTAL

Preparation of ice samples

Preparation of synthetic $MgSO_4 \cdot 11H_2O$ has been extensively described by Genceli and others (2007).

Samples of the top (surface) section of the sea ice and 362 m depth Antarctic ice samples were prepared by cutting with a bandsaw into $10 \times 10 \times 3$ mm^3 pieces. The upper and lower sides of the samples were then flattened (polished) with a microtome in a clean cold chamber at –15°C.

Micro-Raman spectroscopy

Determination of the chemical composition of the inclusions in both ice samples by direct methods was difficult to achieve due to the extremely small size of the crystals (a few μm) and their low material content and high solubilities in water. Therefore, cyro-micro-Raman spectroscopy was employed as the most powerful technique to identify the inclusions inside the ice samples. Spectra of synthetic $MgSO_4 \cdot 11H_2O$ were compared with the observed spectra of the inclusions.

A Jobin-Yvon T64000 triple monochromator equipped with a charge-coupled device (CCD) detector was used to obtain backscattered micro-Raman spectra. Prepared ice samples were placed into the cold chamber on an *x*-*y* translation stage of the microscope. Cooling was achieved indirectly by N_2 gas circulation (at 1 bar) through the chamber, keeping the sample temperature at -15 ± 0.5°C (at 5% relative humidity) for sea ice and at –50°C (at <5% relative humidity) for Antarctic core ice. A laser beam (514.5 nm, 100 mW) was focused to a diameter of ~1 μm on the specimen using a long-working-distance objective lens with 6 mm focal length (Mitutoyo, M Plan Apo 100×). The absolute frequency of the monochromator was calibrated with neon emission lines. The spectral resolution was ~1 cm^{-1} in the range 100–4000 cm^{-1} with a detection time of 60 s. For this analysis, four pieces of sea ice and Antarctic ice-core samples were prepared. We measured 30–40 micro-inclusions per sample.

RESULTS

The inclusions in sea ice were typically 5–20 μm, while those in Antarctic core ice were typically 1–5 μm in diameter (Fig. 1). Most of the inclusions were embedded within the ice grains. The $MgSO_4 \cdot 11H_2O$ inclusions were identified by comparing the observed micro-Raman spectra with those of synthetic $MgSO_4 \cdot 11H_2O$ samples. Other inclusions of, for example, sulfate, nitrate and acid salts were also detected, but discussion of these is beyond the scope of this paper.

Micro-Raman spectra for low-frequency (100–2000 cm^{-1}) and high-frequency (2000–4000 cm^{-1}) ranges of synthetic $MgSO_4 \cdot 11H_2O$, mirabilite and typical meridianiite inclusions in sea ice and Antarctic core ice are presented in Figures 2 and 3. As the inclusions were located in the ice matrix, the dominant ice bands could not be removed from the spectra. Thus, ice spectra are also presented in Figures 2 and 3 for comparison. Due to the small sizes of Antarctic core ice inclusions, it was not possible to measure the complete spectrum from a single inclusion. Therefore the higher-frequency range spectrum (for incorporated water in the lattice and for intracrystalline water bands) of the inclusions introduced in Figure 2 could not be collected and given in Figure 3.

The frequencies, intensities and assignment of the majority of the bands in the micro-Raman spectra of synthetic $MgSO_4 \cdot 11H_2O$, sea-ice and Antarctic core-ice inclusions, ice and mirabilite are presented in Table 1 for comparison. The band identifications are based on literature data.

Micro-Raman spectroscopy of sea-ice inclusions

About 5% of the inclusions detected in sea ice were meridianiite. Significant similarities between the micro-

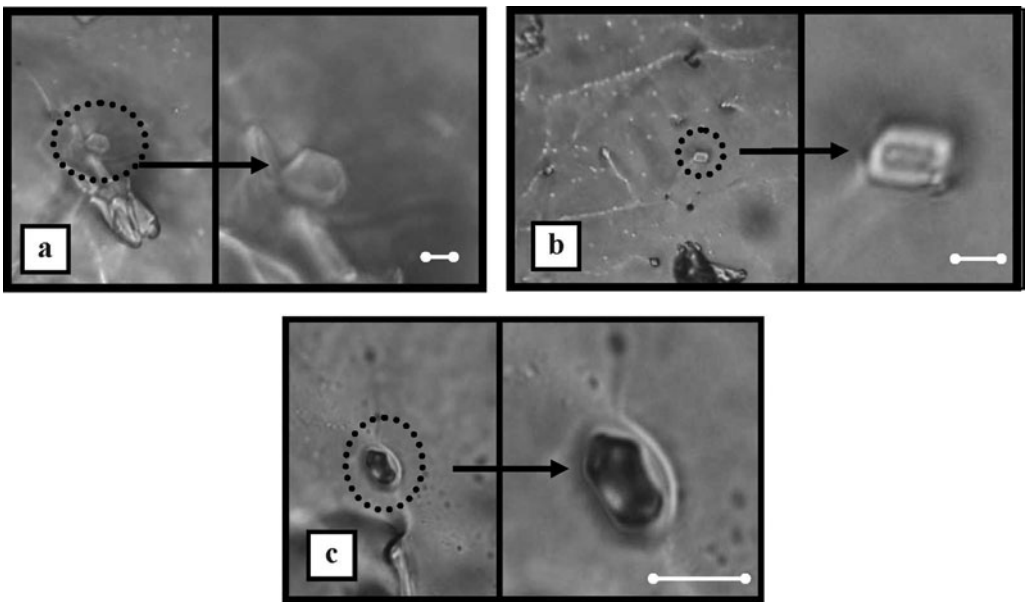

Fig. 1. Optical images of meridianiite inclusion, taken by micro-Raman spectroscopy camera: (a, b) meridianiite inclusions in sea ice; (c) meridianiite inclusions in Antarctic core ice. The scale bar in each image is 5 μm.

Raman spectra of the sea-ice inclusions and the synthetic $MgSO_4 \cdot 11H_2O$ crystals are observed in the SO_4 spectral region. Bands in the synthetic $MgSO_4 \cdot 11H_2O$ crystals ν_1 mode (very strong symmetric stretching vibration) at 990 cm^{-1}, ν_2 mode at 444 cm^{-1} and also a weak peak at 457 cm^{-1}, ν_3 mode at 1116 and 1070 cm^{-1} and ν_4 mode at 619 cm^{-1} have also been observed in the sea-ice inclusions. Due to the water involvement in the hydrogen bonding, the stretching modes of crystal water in the lattice are manifested as a complex band in the 3000–3600 cm^{-1} region, with a maximum at 3393 cm^{-1} for synthetic $MgSO_4 \cdot 11H_2O$ crystals and 3400 cm^{-1} for sea-ice inclusions with several similar shoulders. The water bendings are observed at 1673 cm^{-1} both for synthetic $MgSO_4 \cdot 11H_2O$ crystals and sea-ice inclusions (Table 1). Note that in the micro-Raman spectra of sea-ice inclusion, extra water bands due to the presence of ice surrounding the inclusions are detected at 3265, 3141 and 2188 cm^{-1}, which have also been observed for sea ice in close frequencies. The band of the O–H...O (sulfate) vibration located at 232 cm^{-1} for synthetic $MgSO_4 \cdot 11H_2O$ is not detectable in sea-ice inclusions as it is hidden by the presence of a strong ice-stretching band at 215 cm^{-1} with a resolved mode at 294 cm^{-1}. The O–Mg–O band for sea-ice inclusions seems to be located at 188 cm^{-1}, analogous to that for synthetic $MgSO_4 \cdot 11H_2O$ crystals.

In summary, the excellent micro-Raman spectra vibrational harmony between the synthetic $MgSO_4 \cdot 11H_2O$ and the inclusions of sea-ice samples proves the natural occurrence of meridianiite as a mineral in sea ice. The daughter minerals in inclusions of sea ice may have been formed through freezing of sea ice followed by concentration of brine captured in the ice and the meridianiite crystallization out of this brine. Peterson and others (2007) have also reported the natural occurrence of meridianiite, located in a tree trunk on the surface of a frozen pond in central British Columbia, Canada. Meridianiite has now been recognized as a valid mineral species by the International Mineralogical Association (IMA) Commission, where powder diffraction and physical properties data have been deposited. The crystal structure data of meridianiite have been presented by Peterson and Wang (2006), Genceli and others (2007), and Peterson and others (2007).

Micro-Raman spectroscopy of Antarctic ice inclusions

Magnesium sulfate inclusions in Holocene ice-core samples from Dome Fuji were reported by Ohno and others (2005). We have now investigated these Antarctic ice-core samples using micro-Raman spectroscopy. About 3% of the inclusions detected in the Antarctic core ice were meridianiite. As seen in the typical spectra presented in Figure 2, the most significant peak is the SO_4^{2-} associated symmetric stretching band ν_1 registered at 990 cm^{-1}, and the sulfate modes ν_2 at 446 cm^{-1}, ν_3 at 1117 cm^{-1} and ν_4 at 621 cm^{-1} are all in accordance with the literature data (Table 1). The ν_3 sulfate mode around 1070 cm^{-1} is not clear in Antarctic core-ice inclusions and the assignment of this band was not possible. As with the sea-ice inclusions, the strong ice-stretching band at 215 cm^{-1} with a resolved mode at 286 cm^{-1} hides the band of O–H...O (sulfate) vibration located at 232 cm^{-1}.

The micro-Raman spectra for low vibrations of Antarctic core-ice inclusions compare well with the synthetic $MgSO_4 \cdot 11H_2O$. This suggests that micro-inclusions of $MgSO_4$ salt preserved inside Antarctic core ice almost certainly contain meridianiite. Meridianiite possibly formed as inclusions in Antarctic core ice by the reaction of acid-gas particles (H_2SO_4 and HNO_3) with sea-salt aerosols or terrestrial dusts during their transport through the atmosphere as well as within the snowpack (Röthlisberger and others, 2000; Ohno and others, 2006).

Micro-Raman spectroscopy of mirabilite

By scanning sea-ice and Antarctic core-ice samples by micro-Raman spectroscopy, mirabilite ($Na_2SO_4 \cdot 10H_2O$) was found to be the most common mineral encountered in the inclusions. Figures 2 and 3 and Table 1 present the spectrum of synthetic mirabilite and the band assignments. In order to distinguish between inclusions of $MgSO_4 \cdot 11H_2O$

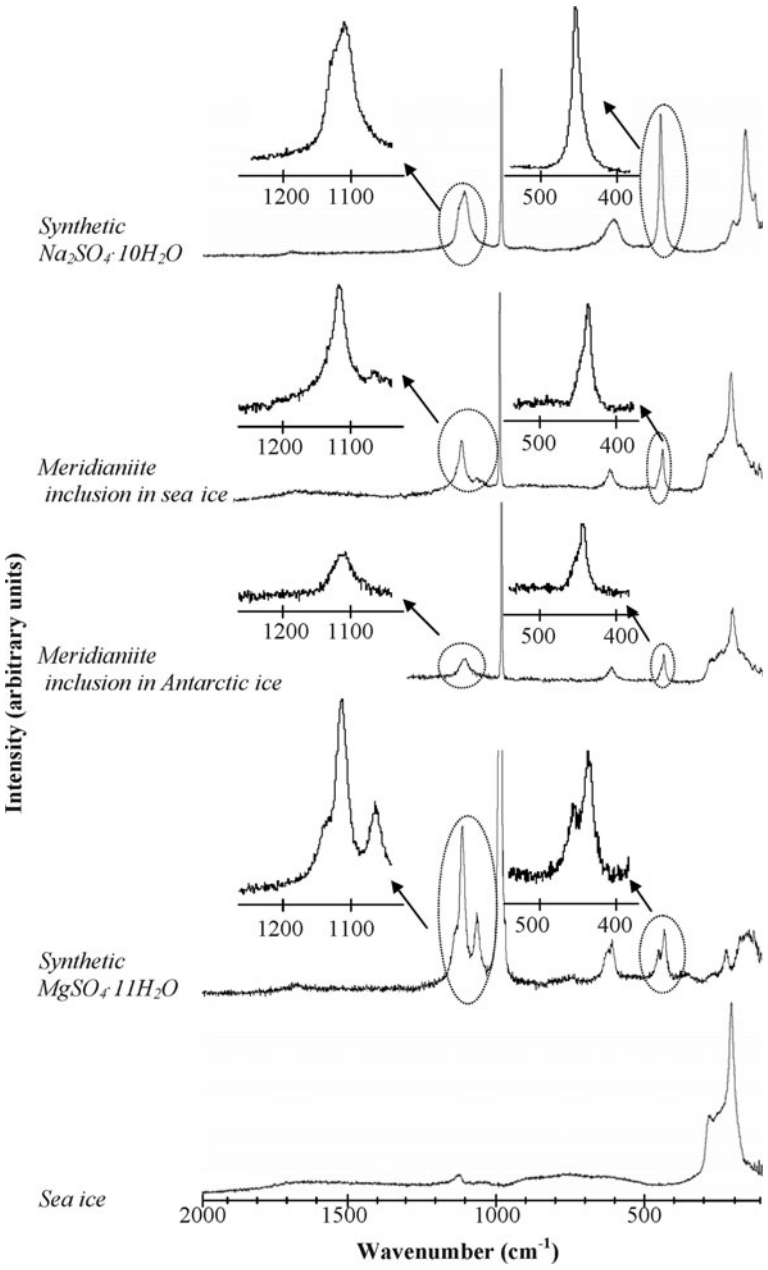

Fig. 2. Low-frequency range Raman spectra.

(denoted as $MgSO_4 \cdot 12H_2O$ by Ohno and others, 2005) and $Na_2SO_4 \cdot 10H_2O$ in Holocene ice-core samples from Dome Fuji, Ohno and others (2005) measured the 300–1500 cm^{-1} wavelength range and used the symmetric stretching SO_4^{2-} band (~990 cm^{-1}) as an indication of the inclusion composition. They distinguished the two salts with a slight shift (1 cm^{-1}) of the main peak: 990 cm^{-1} for mirabilite and 989 cm^{-1} for $MgSO_4{\cdot}11H_2O$. Since the band in the region of 990 cm^{-1} belongs to the symmetric ν_1 stretching mode of the sulfate ion contained in both salts, we consider it desirable to measure more bands if we are to distinguish between meridianiite and mirabilite inclusions.

In this work, mirabilite micro-Raman spectra were collected under atmospheric pressure in a cooling chamber at –15°C, providing the same conditions applied to meridianiite. The spectra of meridianiite and mirabilite harmonize at the SO_4^{2-} symmetric stretching band at 990 cm^{-1}. We can conclude that it is indeed useful to measure a wider spectrum range to distinguish between sulfate salts. Examples of discriminating bands of mirabilite are the υ_2 mode at 456 cm^{-1}, the υ_3 mode at 1112 and 1127 cm^{-1} and the υ_4 mode at 613 cm^{-1} (Murugan and others, 2000). Mirabilite's O–H-band located at wavenumbers between 3100 and 3700 cm^{-1} has a maximum at 3441 cm^{-1} due to stretching water mode incorporated in the lattice (Xu and Schweiger, 1999). Since detailed mirabilite Raman spectrum indexing is not readily available in the literature, not all peaks have been elaborated on in this work. However, by using our findings, it can be concluded that meridianiite has been identified in sea ice and Antarctic core ice.

CONCLUSIONS

The mineral meridianiite was found in sea-ice inclusions from Lake Saroma. The excellent micro-Raman spectra match between the Japanese sea-ice daughter crystals and synthetic $MgSO_4 \cdot 11H_2O$ crystals is presented as evidence of its existence.

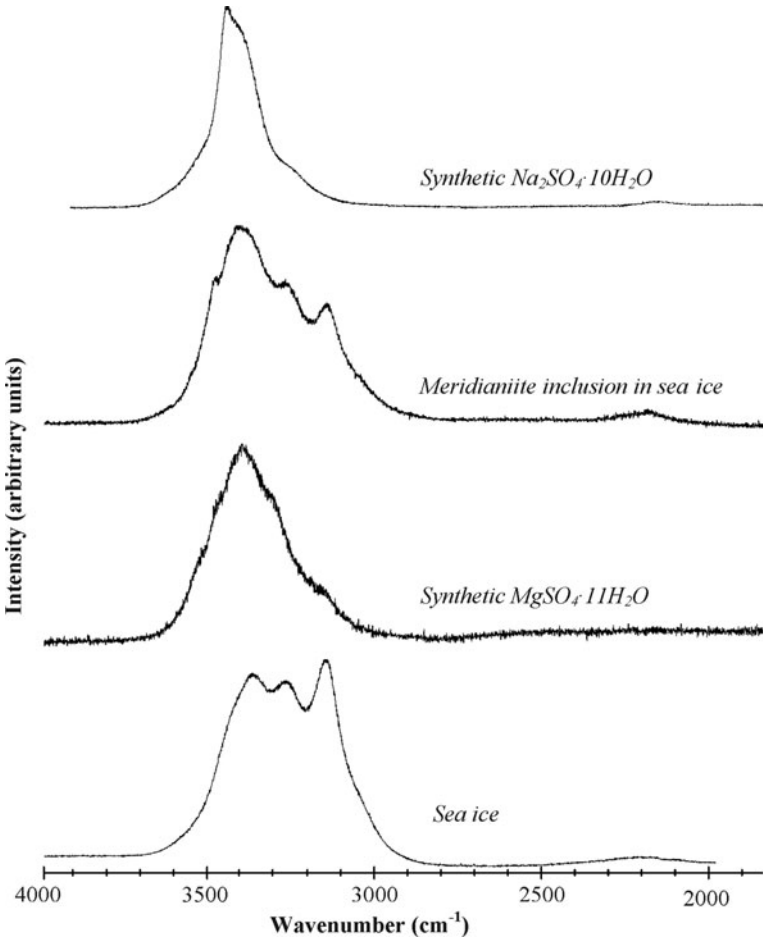

Fig. 3. High-frequency range Raman spectra.

Table 1. The frequency, intensity and assignment of the majority of the bands in the micro-Raman spectra of synthetic $MgSO_4 \cdot 11H_2O$, sea-ice inclusion, Antarctic core-ice inclusion, ice and mirabilite (Prask and Boutin, 1966; Murugan and others, 2000; Socrates, 2001; Makreski and others, 2005; Genceli and others, 2007)

Assignment	Synthetic $MgSO_4 \cdot 11H_2O$ (meridianiite)	Sea-ice inclusion	Antarctic ice inclusion	Ice	Synthetic $Na_2SO_4 \cdot 10H_2O$ (mirabilite)
ν_1 (SO_4)	990 vs	990 vs	990 vs	–	990 vs
ν_2 (SO_4)	444 m	445 m	446 m	–	456 s
	457 w	458 sh	454 sh		
ν_3 (SO_4)	1116 s	1117 m	1117 m	–	1112 m
					1127 sh
ν_3 (SO_4)	1070 m	1071 w	ND	–	–
ν_4 (SO_4)	619 m	621 m	621 m	–	613 m
T(O–H. . .O)	232 m	ND	ND	–	–
δ(O–Mg–O)	188 w	188 w	183 w	–	–
ν(H–O–H)	3393 s	3400 s	NM	–	3441 vs
	3521 sh	3545 sh			3520 sh
	3470 sh	3473 sh			3262 sh
	3304 sh	3303 sh			
	3151 sh				
δ(H–O–H)	1673 w	1673 w	NM	–	–
Ice low-frequency band	–	215 s	215 s	215 s	–
		294 m	286 m	292 m	–
Ice high-frequency band	–	3265 sh	NM	3266 s	–
		2188 w		3141 s	–
		3141 s		2187 w	–

ND: not detected; NM: not measured; s: strong; w: weak; m: medium; sh: shoulder; v: very; ν_1: stretching-mode frequency; ν_2: doubly degenerate bending-mode frequency; ν_3: triply degenerate stretching-mode frequency; ν_4: triply degenerate bending-mode frequency.

Antarctic core-ice inclusions from Dome Fuji match well with the micro-Raman spectra for low vibrations of synthetic $MgSO_4 \cdot 11H_2O$, pointing to the existence of meridianiite in Antarctic continental ice. The extremely small size of the inclusions (1–5 μm) was the greatest obstacle to measuring the whole micro-Raman spectrum from a single inclusion.

The Raman spectrum of $MgSO_4 \cdot 11H_2O$ (meridianiite) showed significant differences from that of $Na_2SO_4 \cdot 10H_2O$ (mirabilite).

ACKNOWLEDGEMENT

We thank E. Burke, Chairman of IMA Commission on New Minerals, for support and help during this work.

REFERENCES

Baker, I. and D. Cullen. 2003. SEM/EDS observations of impurities in polar ice: artifacts or not? *J. Glaciol.,* **49**(165), 184–190.

Barnes, P.R.F. and E.W. Wolff. 2004. Distribution of soluble impurities in cold glacial ice. *J. Glaciol.,* **50**(170), 311–324.

Dome-F Deep Coring Group. 1998. Deep ice-core drilling at Dome Fuji and glaciological studies in east Dronning Maud Land, Antarctica. *Ann. Glaciol.,* **27**, 333–337.

EPICA Community Members. 2004. Eight glacial cycles from an Antarctic ice core. *Nature,* **429**(6992), 623–628.

Fritzsche, C.J. 1837. Ueber eine neue Verbindung der schwefelsauren Talkerde mit Wasser. *Poggendorffs Ann. Physik Chemie,* **42**, 577–580.

Genceli, F.E., A.L. Lutz, A.L. Spek and G.-J. Witkamp. 2007. Crystallization and characterization of a new magnesium sulphate $MgSO_4 \cdot 11H_2O$. *Cryst. Growth Design,* **7**(12), 2460–2466.

Jouzel, J. 2003. Climat du passé (400 000 ans): des temps géologiques à la dérive actuelle. *C. R. Geosci.,* **335**(6–7), 509–524.

Jouzel, J. *and 13 others*. 1989. Global change over the last climatic cycle from the Vostok ice core record (Antarctica). *Quat. Int.,* **2**, 15–24.

Jouzel, J., C. Lorius and D. Raynaud. 2006. Climat et atmosphre au Quaternaire: de nouveaux carottages glaciaires. *C. R. Palevol,* **5**(1–2), 45–55.

Kawamura, T., K. Shirasawa, M. Ishikawa, T. Takatsuka, T. Daibou and M. Leppäranta. 2004. On the annual variation of characteristics of snow and ice in Lake Saroma. *In 17th International Symposium on Ice, 21–25 June 2004. Saint Petersburg, Russia. Proceedings,* Madrid, International Association of Hydraulic Engineering and Research, 212–220.

Legrand, M. and P. Mayewski. 1997. Glaciochemistry of polar ice cores: a review. *Rev. Geophys.,* **35**(3), 219–243.

Makreski, P., G. Jovanovski and S. Dimitrovska. 2005. Minerals from Macedonia XIV. Identification of some sulfate minerals by vibrational (infrared and Raman) spectroscopy. *Vib. Spectrosc.,* **39**(2), 229–239.

Murugan, R., A. Ghule and H. Chang. 2000. Thermo-Raman spectroscopic studies on polymorphism in Na_2SO_4. *J. Phys. Cond. Matter,* **12**(5), 677–700.

Ohno, H., A. Igarashi and T. Hondoh. 2005. Salt inclusions in polar ice core: location and chemical form of water-soluble impurities. *Earth Planet. Sci. Lett.,* **232**(1–2), 171–178.

Ohno, H., M. Igarashi and T. Hondoh. 2006. Characteristics of salt inclusions in polar ice from Dome Fuji, East Antarctica. *Geophys. Res. Lett.,* **33**(8), L08501. (10.1029/2006GL025774.)

Peterson, R.C. and R. Wang. 2006. Crystal molds on Mars: melting of a possible new mineral species to create Martian chaotic terrain. *Geology,* **34**(11), 957–960.

Peterson, R.C., W. Nelson, B. Madu and H.F. Shurvell. 2007. Meridianiite: a new mineral species observed on Earth and predicted to exist on Mars. *Am. Mineral.,* **92**(10), 1756–1759.

Petit, J.R. *and 18 others*. 1999. Climate and atmospheric history of the past 420 000 years from the Vostok ice core, Antarctica. *Nature,* **399**(6735), 429–436.

Prask, H.J. and H. Boutin. 1966. Low-frequency motions of H_2O molecules in crystals. III. *J. Chem. Phys.,* **45**(9), 3284–3295.

Röthlisberger, R., M.A. Hutterli, S. Sommer, E.W. Wolff and R. Mulvaney. 2000. Factors controlling nitrate in ice cores: evidence from the Dome C deep ice core. *J. Geophys. Res.,* **105**(D16), 20,565–20,572.

Sinha, N.K. 1977. Technique for studying structure of sea ice. *J. Glaciol.,* **18**(79), 315–323.

Socrates, G. 2001. *Infrared and Raman characteristic group frequencies: tables and charts. Third edition*. Chichester, John Wiley & Sons.

Wakatsuchi, M. and T. Kawamura. 1987. Formation processes of brine drainage channels in sea ice. *J. Geophys. Res.,* **92**(C7), 7195–7197.

Weeks, W.F. and S.F. Ackley. 1982. The growth, structure, and properties of sea ice. *CRREL Monogr.* 82-1.

Xu, B. and G. Schweiger. 1999. *In-situ* Raman observation of phase transformation of Na_2SO_4 during the hydration/dehydration cycles on single levitated microparticle. *J. Aerosol Sci.,* **30**, Suppl. 1, S379–S380.

MS received 29 September 2007 and accepted in revised form 22 August 2008